## The effects of the Earth's mass centric variations and figure polar shifts

The Earth's mass centric coordinates and figure polar coordinates are both important geodetic elements with both geometric and physical properties. In the Earth-fixed coordinate system with arbitrary positioning and orientation, the mass centric coordinates of the deforming Earth can be uniquely determined by the degree-1 geopotential coefficients $(\bar{C}_{10}, \bar{C}_{11}, \bar{S}_{11})$, and the mechanical figure polar coordinates of the deforming Earth can be uniquely determined by the degree-2 tesseral harmonic geopotential coefficients $(\bar{C}_{21}, \bar{S}_{21})$. Therefore, the various tidal and non-tidal effects on Earth's center of mass and figure pole can be accurately obtained in geodesy.

### 8.5.1 The tidal effects on the Earth's center of mass and figure pole

The tidal effects on the Earth's center of mass and figure pole are determined by the tidal effects on the degree-1 and degree-2 order 1 geopotential coefficients, respectively. The figure polar tidal effect are the sum of the body and load tidal effect of all the degree-2 diurnal tidal wave.

#### (1) Tidal effect prediction calculation on the Earth's mass centric variations

The solid Earth tide is derived on basis of the mechanical balance theory of the celestial gravitation and centrifugal force. The Earth's tidal force from the celestial body at the Earth's center of mass is always equal to zero, so geodesy does not specifically study the solid tidal effect on the Earth's center of mass. Ocean tides and surface atmosphere tides lead to the redistribution of surface mass, causing periodic variations of Earth's center of mass.

Section 8.4 has introduced the spherical harmonic synthesis algorithm for ocean and surface atmosphere tidal load effects. From the degree-1 spherical harmonic coefficient of each tidal constituent $\sigma_j$ in the load tidal spherical harmonic coefficient model, including the in-phase and out-of-phase amplitudes of the degree-1 term, the variations of Earth's center of mass caused by the tidal constituent $\sigma_j$ at any epoch time can be calculated. After that, the contributions of all the tidal constituents are superimposed, which is the tidal load effects on the Earth's mass centric variations at the epoch time.

Assuming that the in-phase and out-of-phase amplitudes of the degree-1 tidal load spherical harmonic coefficients of the tidal constituent $\sigma_j$ are $\left(\Delta\bar{C}_{10}^{j+}, \Delta\bar{C}_{11}^{j+}, \Delta\bar{S}_{11}^{j+}\right)$ and $\left(\Delta\bar{C}_{10}^{j-},\ \Delta\bar{C}_{11}^{j-},\ \Delta\bar{S}_{11}^{j-}\right)$, respectively, and considering that the degree-1 load potential Love number is equal to zero, $k_1' \equiv 0$, then at any epoch time $t$, the tidal load effects on the Earth's mass centric variations can be expressed as:

$$\begin{cases}\Delta x_{cm}(t) = \sqrt{3}R\frac{\rho_w}{\rho_e}\sum_{j=1}^{n}\left[\Delta\bar{C}_{11}^{j+}cos\left(\phi_j(t)+\varepsilon_j\right) + \Delta\bar{C}_{11}^{j-}sin\left(\phi_j(t)+\varepsilon_j\right)\right] \\ \Delta y_{cm}(t) = \sqrt{3}R\frac{\rho_w}{\rho_e}\sum_{j=1}^{n}\left[\Delta\bar{S}_{11}^{j+}cos\left(\phi_j(t)+\varepsilon_j\right) + \Delta\bar{S}_{11}^{j-}sin\left(\phi_j(t)\right)+\varepsilon_j\right] \\ \Delta z_{cm}(t) = \sqrt{3}R\frac{\rho_w}{\rho_e}\sum_{j=1}^{n}\left[\Delta\bar{C}_{10}^{j+}cos\left(\phi_j(t)+\varepsilon_j\right) + \Delta\bar{C}_{10}^{j-}sin\left(\phi_j(t)+\varepsilon_j\right)\right]\end{cases} \quad (5.1)$$

Where, $\phi_j(t)$ is the astronomical argument of the tidal constituent $\sigma_j$ at the epoch time $t$,

$\varepsilon_j$ is the phase bias of $\sigma_j$, $n$ is the number of tidal constituents in the tidal load spherical harmonic coefficient model, e.g. the 720-degree ocean tidal load spherical harmonic coefficient model FES2014b720cs.dat constructed in Section 8.2.3 has 34 tidal constituents including degree-1 terms $(n = 34)$, and the 360-degree surface atmosphere tidal load spherical harmonic coefficient model ECMWF2006n360cs.dat constructed in Section 8.2.4 has 4 tidal constituents including degree-1 terms $(n = 4)$.

Here, from the in-phase and out-of-phase amplitudes of the degree-1 terms of 34 tidal constituents in the model FES2014b720cs.dat in section 8.2.3, the ocean tidal load effect time series on the Earth's mass centric variations are calculated as shown in Fig 5.1. The time span of the time series is from July 1, 2016 to July 15, 2016, with a time interval of 30 minutes.

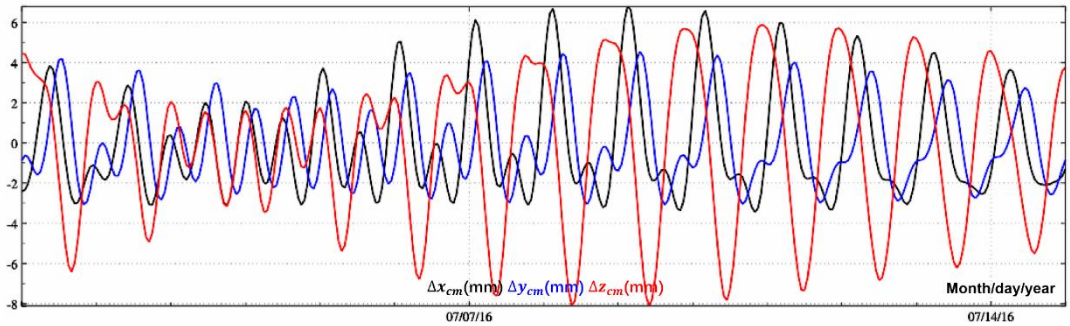


**Fig 5.1 The ocean tidal load effect time series on the Earth's mass centric variations**

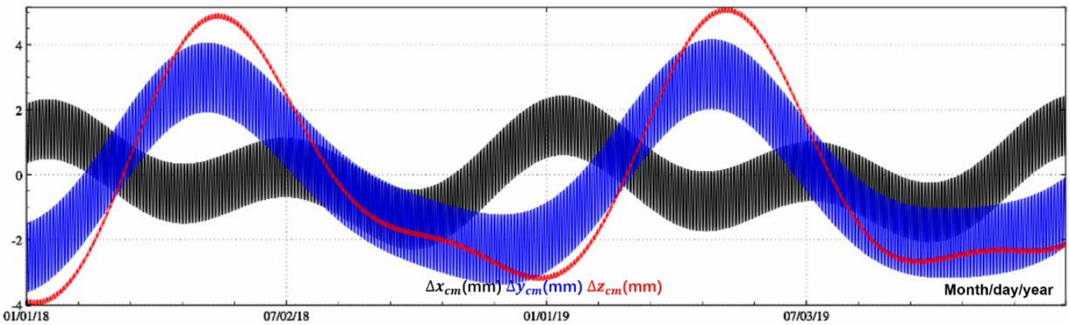


**Fig 5.2 The surface atmosphere tidal load effect time series on the Earth's mass centric variations**

Here, from the in-phase and out-of-phase amplitudes of the degree-1 terms of 4 tidal constituents in the model ECMWF2006n360cs.dat in section 8.2.4, the surface atmosphere tidal load effect time series on the Earth's mass centric variations are calculated as shown in Fig 5.2. The time span of the time series is from January 1, 2018 to December 31, 2019 (2 years), with a time interval of 4 hours.

For ocean or surface atmosphere tidal load models constructed from different sources of observations, the load tidal effects on the Earth's mass centric variations may have some small differences.

**(2) Tidal effect prediction calculation on the Earth's figure polar shift**

The rigorous algorithm formulas for determining the figure polar shift $(\Delta x_{sfp}, -\Delta y_{sfp})$ from the degree-2 tesseral harmonic geopotential coefficient variations $(\Delta\bar{C}_{21}, \Delta\bar{S}_{21})$ with the geopotential coefficients $(\bar{C}_{20}, \bar{S}_{22})$ are as follows:

$$\Delta x_{sfp} = -\frac{\sqrt{3}b}{\bar{C}_{20}}\Delta\bar{C}_{21} - \frac{6\bar{S}_{22}b}{(\bar{C}_{20})^2}\Delta\bar{S}_{21},\quad \Delta y_{sfp} = +\frac{\sqrt{3}b}{\bar{C}_{20}}\Delta\bar{S}_{21} - \frac{6\bar{S}_{22}b}{(\bar{C}_{20})^2}\Delta\bar{C}_{21} \tag{5.2}$$

Where, $b$ is the short semi-axis of the Earth, $\Delta\bar{C}_{21}, \Delta\bar{S}_{21}$ take the approximate mean value.

The solid Earth tidal effects on the degree-2 tesseral harmonic geopotential coefficients in Section 8.1, namely the degree-2 diurnal body tide cluster $(\Delta\bar{C}_{21}, \Delta\bar{S}_{21})$, characterize the solid tidal effects on the Earth's figure pole. There are frequency dependent in the degree-2 diurnal poetential Love number of the rotating microellipsoidal Earth (48 degree-2 diurnal tidal constituents are corrected for frequency, as shown in Tab 1.7). The solid Earth tidal effects on Earth's figure polar shift can be calculated from solid tidal effect on the degree-2 tesseral harmonic geopotential coefficients of 48 degree-2 diurnal tidal constituents.

Similar to the load tidal effects on the Earth's mass centric variations, the algorithm formulas for predicting the load tidal effects on the Earth's figure polar shift can be derived from the degree-2 tesseral load tidal spherical harmonic coefficients:

$$\Delta x_{sfp} = -\frac{3\rho_w}{5\rho_e}\frac{b(1+k_2')}{\bar{C}_{20}}\begin{pmatrix} \sqrt{3}\sum_{j=1}^{n}\left[\Delta\bar{C}_{21}^{j+}cos\left(\phi_j(t)+\varepsilon_j\right) + \Delta\bar{C}_{21}^{j-}sin\left(\phi_j(t)+\varepsilon_j\right)\right] \\ +\frac{6\bar{S}_{22}}{\bar{C}_{20}}\sum_{j=1}^{n}\left[\Delta\bar{S}_{21}^{j+}cos\left(\phi_j(t)+\varepsilon_j\right) + \Delta\bar{S}_{21}^{j-}sin\left(\phi_j(t)+\varepsilon_j\right)\right] \end{pmatrix} \tag{5.3}$$

$$\Delta y_{sfp} = \frac{3\rho_w}{5\rho_e}\frac{b(1+k_2')}{\bar{C}_{20}}\begin{pmatrix} \sqrt{3}\sum_{j=1}^{n}\left[\Delta\bar{S}_{21}^{j+}cos\left(\phi_j(t)+\varepsilon_j\right) + \Delta\bar{S}_{21}^{j-}sin\left(\phi_j(t)+\varepsilon_j\right)\right] \\ -\frac{6\bar{S}_{22}}{\bar{C}_{20}}\sum_{j=1}^{n}\left[\Delta\bar{C}_{21}^{j+}cos\left(\phi_j(t)+\varepsilon_j\right) + \Delta\bar{C}_{21}^{j-}sin\left(\phi_j(t)+\varepsilon_j\right)\right] \end{pmatrix} \tag{5.4}$$

Where, $\bar{C}_{21}^{j+}, \Delta\bar{C}_{21}^{j-}, \Delta\bar{S}_{21}^{j+}, \Delta\bar{S}_{21}^{j-}$ are the in-phase and out-of-phase amplitudes of the degree-1 order-1 tidal load spherical harmonic coefficients of the tidal constituent $\sigma_j$, respectively, $n$ is the number of tidal constituents in the tidal load spherical harmonic coefficient model, for the model FES2014b720cs.dat, $n = 34$.

Using the same numerical standard and ocean tidal load effect algorithm on geopotential coefficients in section 8.2.3, the ocean tidal load effect (in unit of m) time series on the figure polar shift from January 1, 2019 to February 28, 2019 is calculated by the ocean tidal load model FES2014b720cs.dat (34 tidal constituents), with a time interval of 30 minutes, as shown in Fig 5.3.

Fig 5.3 shows that the ocean tidal load effects on the Earth's figure pole shift are dominated by diurnal variation, and the difference between the maximum and minimum values is more than 40m in one month.

Using the same numerical standard and surface atmosphere tidal load effect algorithm on geopotential coefficients in section 8.2.4, the surface atmosphere tidal load effect (in unit of m) time series on the figure polar shift from January 1, 2018 to January 31, 2019 is calculated by the surface atmosphere tidal load model ECMWF2006n360cs.dat (4 tidal constituents), with a time interval of 4 hours, as shown in Fig 5.4.

Fig 5.4 shows that the surface atmosphere tidal load effect on the Earth's figure polar shift are dominated by diurnal variation in the short peroid, and the amplitude is decimeter level. The annual amplitude is large, and the difference between the maximum and minimum values is more than 7m.

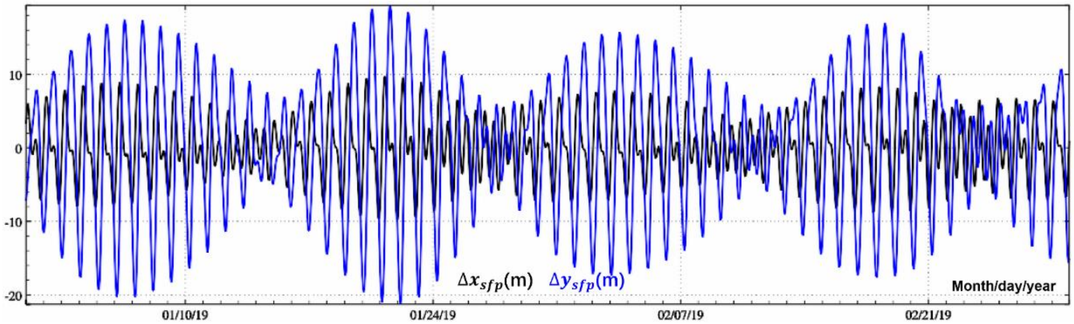


**Fig 5.3 The ocean tidal load effect time series on Earth's figure polar shift in ITRS**

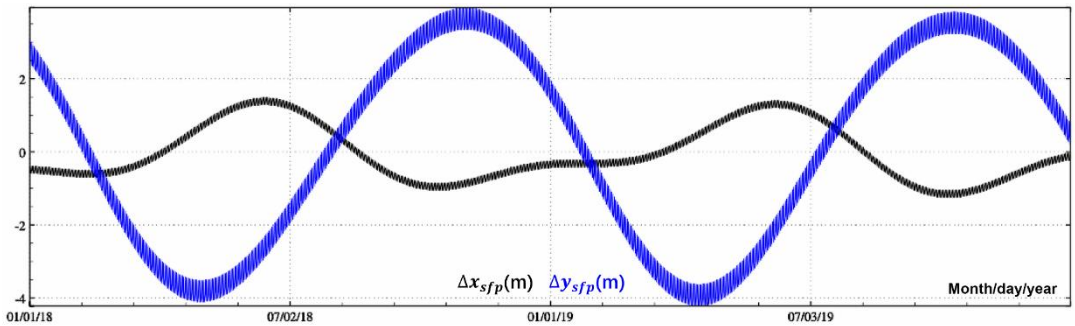


**Fig 5.4 The surface atmosphere tidal load effect time series on Earth's figure polar shift in ITRS**

### 8.5.2 The load effects on the Earth's center of mass and figure pole

Section 8.2 has introduced the non-tidal load spherical harmonic synthesis algorithm for the change of the Earth's gravity field, including the load effect calculation of the sea level variations, surface atmosphere variations and land water variations. Among them, the degree-1 load spherical harmonic coefficient variations in the non-tidal load spherical harmonic model can be employed to calculate the non-tidal load effects on Earth's mass centric variations, and the degree-2 tesseral load spherical harmonic coefficient variations can be employed to calculate the non-tidal load effects on Earth's figure polar shift.

**(1) Calculation of non-tidal load effect on the Earth's mass centric variations**

Assuming that the degree-1 non-tidal load spherical harmonic coefficient variations are

$(\Delta\bar{C}_{10}^{w}, \Delta\bar{C}_{11}^{w}, \Delta\bar{S}_{11}^{w})$, considering $k_1' = 0$, the non-tidal load effect on Earth's mass centric variations can be obtained as follows:

$$\Delta x_{cm} = \sqrt{3}R\frac{\rho_w}{\rho_e}\Delta\bar{C}_{11}^{w}, \quad \Delta y_{cm} = \sqrt{3}R\frac{\rho_w}{\rho_e}\Delta\bar{S}_{11}^{w}, \quad \Delta z_{cm} = \sqrt{3}R\frac{\rho_w}{\rho_e}\Delta\bar{C}_{10}^{w} \tag{5.5}$$

From the degree-1 load spherical harmonic coefficient variation weekly time series $(\Delta\bar{C}_{10}^{sea}, \Delta\bar{C}_{11}^{sea}, \Delta\bar{S}_{11}^{sea})$ in the sea level variation load spherical harmonic coefficient model weekly time series constructed in 8.2.4 section, the Earth's mass centric variation weekly time series (in unit of mm, relative to the mean center of mass in 2018) are calculated according to formula (5.5), and the result is shown in figure 5.5. The time span of the time series is from January 2018 to December 2020.

From the degree-1 load spherical harmonic coefficient variation weekly time series $\left(\Delta\bar{C}_{10}^{air}, \Delta\bar{C}_{11}^{air}, \Delta\bar{S}_{11}^{air}\right)$ in the surface atmosphere variation load spherical harmonic coefficient model weekly time series constructed in 8.2.5 section, the Earth's mass centric variation weekly time series (in unit of mm, relative to the mean center of mass in 2018) are calculated according to formula (5.5), and the result is shown in figure 5.6. The time span of the time series is from January 2018 to December 2020.

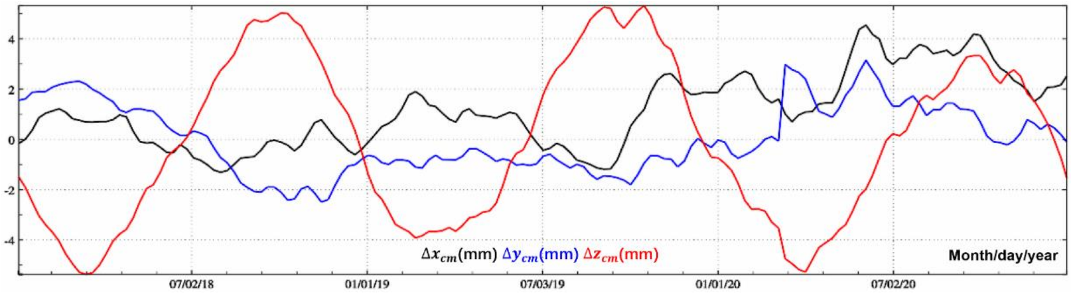


**Fig 5.5 The sea level variation load effect time series on Earth's mass centric variation (relative to the mean center of mass in 2018)**

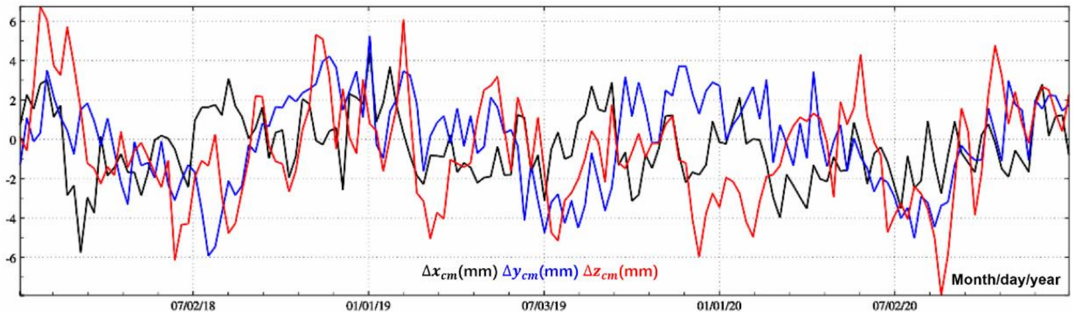


**Fig 5.6 The surface atmosphere variation load effect time series on Earth's mass centric variation (relative to the mean center of mass in 2018)**

From the degree-1 load spherical harmonic coefficient variation weekly time series

$(\Delta\bar{C}_{10}^{lnd}, \Delta\bar{C}_{11}^{lnd}, \Delta\bar{S}_{11}^{lnd})$ in the global land water variation load spherical harmonic coefficient model weekly time series constructed in 8.2.6 section, the Earth's mass centric variation weekly time series (in unit of mm, relative to the mean center of mass in 2018) are calculated according to formula (5.5), and the result is shown in figure 5.7. The time span of the time series is from January 2018 to September 2020.

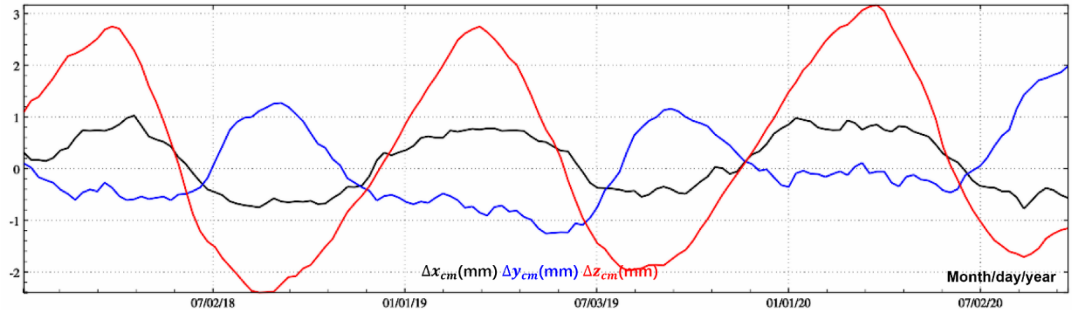


**Fig 5.7 The global land water variation load effect time series on Earth's mass centric variation (relative to the mean center of mass in 2018)**

Fig 5.5 ~ Fig 5.7 show that in the non-tidal load effects on Earth's mass centric variation, the difference between the maximum and minimum values of the load effect of sea level variations reaches 10mm, that of land water variations reaches 5mm, and that of surface atmosphere variations exceeds 10mm.

**(2) Calculation of non-tidal load effect on the Earth's figure polar shift**

The algorithm formula of the degree-2 tesseral non-tidal load spherical harmonic coefficient variations $(\Delta\bar{C}_{21}^{w}, \Delta\bar{S}_{21}^{w})$ expressed by the degree-2 tesseral harmonic geopotential coefficient variations $(\Delta\bar{C}_{21}, \Delta\bar{S}_{21})$ is:

$$\Delta\bar{C}_{21} = \frac{3\rho_w}{5\rho_e}(1+k_2')\Delta\bar{C}_{21}^{w}, \quad \Delta\bar{S}_{21} = \frac{3\rho_w}{5\rho_e}(1+k_2')\Delta\bar{S}_{21}^{w} \tag{5.6}$$

Substituting Formula (5.6) into Formula (5.2), the non-tidal load effect algorithm formulas on the figure polar shift can be obtained from the degree-2 order-1 non-tidal load spherical harmonic coefficient variations $(\Delta\bar{C}_{21}^{w}, \Delta\bar{S}_{21}^{w})$.

$$\Delta x_{sfp} = -\frac{3\rho_w}{5\rho_e}\frac{b}{\bar{C}_{20}}(1+k_2')\left(\sqrt{3}\Delta\bar{C}_{21}^{w} + \frac{6\bar{S}_{22}}{\bar{C}_{20}}\Delta\bar{S}_{21}^{w}\right) \tag{5.7}$$

$$\Delta y_{sfp} = +\frac{3\rho_w}{5\rho_e}\frac{b}{\bar{C}_{20}}(1+k_2')\left(\sqrt{3}\Delta\bar{S}_{21}^{w} - \frac{6\bar{S}_{22}}{\bar{C}_{20}}\Delta\bar{C}_{21}^{w}\right) \tag{5.8}$$

From the degree-2 order-1 sea level variation load spherical harmonic coefficient variation weekly time series $(\Delta\bar{C}_{21}^{sea}, \Delta\bar{S}_{21}^{sea})$ in 8.2.4 section, the Earth's figure polar shift weekly time series (in unit of m, relative to the mean figure pole in 2018) are calculated according to formulas (5.7) and (5.8), and the result is shown in figure 5.8. The time span of the time series is from January 2018 to December 2020.

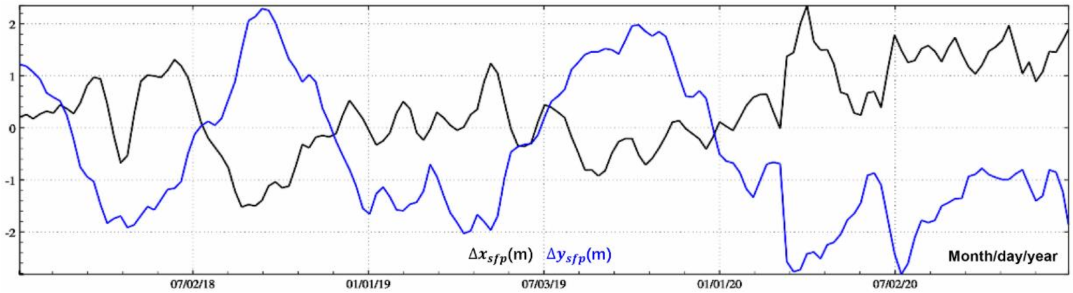


**Fig 5.8 The sea level variation load effect time series on Earth's figure polar shift in ITRS (relative to the mean figure pole in 2018)**

From the degree-2 order-1 surface atmosphere variation load spherical harmonic coefficient variation weekly time series $(\Delta\bar{C}_{21}^{air}, \Delta\bar{S}_{21}^{air})$ in 8.2.5 section, the Earth's figure polar shift weekly time series (in unit of m, relative to the mean figure pole in 2018) are calculated according to formulas (5.7) and (5.8), and the result is shown in figure 5.9. The time span of the time series is from January 2018 to December 2020.

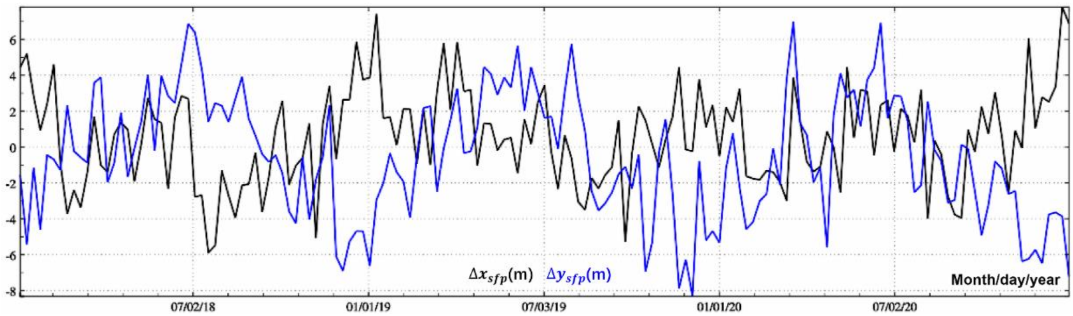


**Fig 5.9 The surface atmosphere variation load effect time series on Earth's figure polar shift in ITRS (relative to the mean figure pole in 2018)**

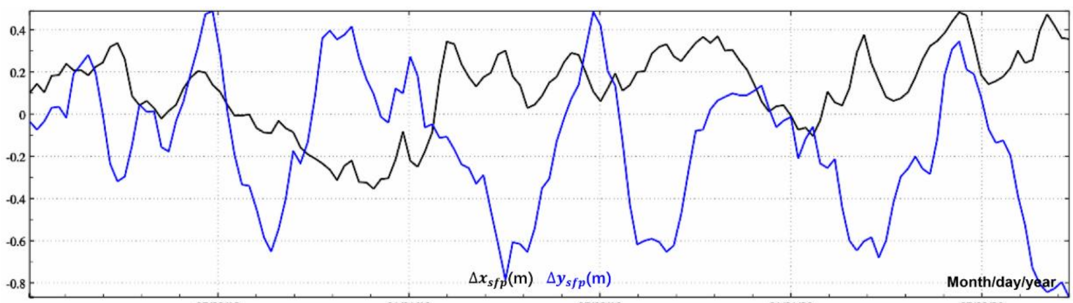


**Fig 5.10 The global land water variation load effect time series on Earth's figure polar shift in ITRS (relative to the mean figure pole in 2018)**

From the degree-2 order-1 global land water variation load spherical harmonic coefficient variation weekly time series $(\Delta\bar{C}_{21}^{lnd}, \Delta\bar{S}_{21}^{lnd})$ in 8.2.6 section, the Earth's figure polar shift weekly time series (in unit of m, relative to the mean figure pole in 2018) are calculated according to formulas (5.7) and (5.8), and the result is shown in figure 5.10. The time span of the time series is from January 2018 to September 2020.

The statistical results show in the non-tidal load effects on Earth's figure polar shift, that the difference between the maximum and minimum values of the load effects of sea level variations is more than 4m, that of global land water variations is 1.2m, and that of surface atmosphere variations is more than 14m.

**8.5.3 Earth's mass centric variation effects on all-element geodetic variations**

The coordinates of the Earth's center of mass are geodetic elements with global spatial scale, and the Earth's center of mass is the degree-1 term of the mechanical equilibrium figure of the deforming Earth. The variations of the Earth's center of mass measured by the SLR have generally removed the ocean and atmosphere tidal load effects, which represent the deformation of whole Earth system excited by the non-tidal load variations, thus affecting various geometric and physical geodetic elements in the whole Earth space, rather than simply showing the ground site displacement of pure geometric elements.

The variations $(\Delta x_{cm}, \Delta y_{cm}, \Delta z_{cm})$ of the Earth's center of mass can be determined by measuring the degree-1 geopotential coefficient variations $(\Delta\bar{C}_{10}, \Delta\bar{C}_{11}, \Delta\bar{S}_{11})$ according to the following formula:

$$\Delta x_{cm} = \sqrt{3}R\Delta\bar{C}_{11}, \quad \Delta y_{cm} = \sqrt{3}R\Delta\bar{S}_{11}, \quad \Delta z_{cm} = \sqrt{3}R\Delta\bar{C}_{10} \tag{5.9}$$

In Formulas (2.8) ~ (2.20), let $n = 1$, considering $\bar{P}_{10}(cos\theta) = \sqrt{3}cos\theta$, $\bar{P}_{11}(cos\theta) = \sqrt{3}\sin\theta$, we can obtain the algorithm formulas of the Earth's mass centric variation effects on geodetic variations from the SLR measured variations of the Earth's center of mass. Among them, the algorithm formula of the Earth's mass centric variation effect on height anomaly at $(r, \theta, \lambda)$ is:

$$\Delta\zeta(r,\theta,\lambda) = \frac{GM}{\gamma r^2}\frac{a}{R}(\Delta x_{cm} cos\lambda sin\theta + \Delta y_{cm} sin\lambda sin\theta + \Delta z_{cm} cos\theta) \tag{5.10}$$

The algorithm formula of the Earth's mass centric variation effect on ground gravity is◉:

$$\Delta g^{s}(r,\theta,\lambda) = \frac{2GM}{r^3}\frac{a}{R}(1 + 2h_1')(\Delta x_{cm} cos\lambda sin\theta + \Delta y_{cm} sin\lambda sin\theta + \Delta z_{cm} cos\theta) \tag{5.11}$$

Where, $h_1'$ is the degree-1 load radial Love number.

The algorithm formula of the Earth's mass centric variation effect on gravity (disturbance) outside the solid Earth is:

$$\Delta g^{\delta}(r,\theta,\lambda) = \frac{2GM}{r^3}\frac{a}{R}(\Delta x_{cm} cos\lambda sin\theta + \Delta y_{cm} sin\lambda sin\theta + \Delta z_{cm} cos\theta) \tag{5.12}$$

The algorithm formula of the Earth's mass centric variation effect on ground tilt is◉:

South: $\Delta\xi^{s}(r,\theta,\lambda) =$

$$\frac{GM}{\gamma r^3}\frac{a}{R}\sin\theta\,(1-h_1')(\Delta x_{cm}cos\theta cos\lambda+\Delta y_{cm}\sin\theta\, sin\lambda-\Delta z_{cm}sin\theta) \quad (5.13)$$

West: $$\Delta\eta^s(r,\theta,\lambda)=\frac{GM}{\gamma r^3}\frac{a}{R}(1-h_1')(\Delta x_{cm}sin\lambda-\Delta y_{cm}cos\lambda) \quad (5.14)$$

The algorithm formula of the Earth's mass centric variation effect on vertical deflection outside the solid Earth is:

South: $$\Delta\xi^s=\frac{GM}{\gamma r^3}\frac{a}{R}\sin\theta\,(\Delta x_{cm}cos\theta cos\lambda+\Delta y_{cm}\sin\theta\, sin\lambda-\Delta z_{cm}sin\theta) \quad (5.15)$$

West: $$\Delta\eta^s(r,\theta,\lambda)=\frac{GM}{\gamma r^3}\frac{a}{R}(\Delta x_{cm}sin\lambda-\Delta y_{cm}cos\lambda) \quad (5.16)$$

The algorithm formula of the Earth's mass centric variation effect on ground site displacement is◉:

East: $$\Delta e(r,\theta,\lambda)=-\frac{GM}{r^2\gamma}\frac{a}{R}l_1'(\Delta x_{cm}sin\lambda-\Delta y_{cm}cos\lambda) \quad (5.17)$$

North: $$\Delta n=-\frac{GM}{r^2\gamma}\frac{a}{R}l_1'sin\theta(\Delta x_{cm}cos\theta cos\lambda+\Delta y_{cm}cos\theta sin\lambda-\Delta z_{cm}sin\theta) \quad (5.18)$$

Radial: $$\Delta r(r,\theta,\lambda)=\frac{GM}{r^2\gamma}\frac{a}{R}h_1'(\Delta x_{cm}cos\lambda sin\theta+\Delta y_{cm}sin\lambda sin\theta+\Delta z_{cm}cos\theta) \quad (5.19)$$

Where, $l_1'$ is the degree-1 load horizontal Love number.

The algorithm formula of the Earth's mass centric variation effect on gravity gradient outside the solid Earth is:

Radial: $$\Delta T_{rr}(r,\theta,\lambda)=\frac{6GM}{r^4}\frac{a}{R}(\Delta x_{cm}cos\lambda sin\theta+\Delta y_{cm}sin\lambda sin\theta+\Delta z_{cm}cos\theta) \quad (5.20)$$

North: $$\Delta T_{NN}(r,\theta,\lambda)=\frac{GM}{r^4}\frac{a}{R}(\Delta x_{cm}cos\lambda sin\theta+\Delta y_{cm}sin\lambda sin\theta+\Delta z_{cm}cos\theta) \quad (5.21)$$

West: $$\Delta T_{WW}(r,\theta,\lambda)=\frac{GM}{r^4}\frac{a}{R}(\Delta x_{cm}sin\lambda+\Delta y_{cm}cos\lambda) \quad (5.22)$$

In the above expressions, the Earth's mass centric variation effects on the geodetic variations marked ◉ are valid only when their sites are fixed with the solid Earth, and that on the remaining geodetic variations are suitable on the ground or outside the solid Earth.

In the following, using the Earth's mass centric variation time series from Center for Space Research in University of Texas in USA (UT/CSR) from LAGEOS-1/2, Stella, Starlette, AJISAI, BEC and LARES Satellite Laser Ranging (SLR) measured, the Earth's mass centric variation effect time series on various geodetic elements at the ground point P (105°E, 32°N, H720m) are calculated according to the formulas (5.10) ~ (5.22) as shown in Fig 5.11 and Fig 5.12, with the mean radius $R=6371000$m of the Earth and $h_1'$ =-0.2871, $l_1'$ =0.1045. The time span of the time series is from January 2018 to December 2022 (5 years).

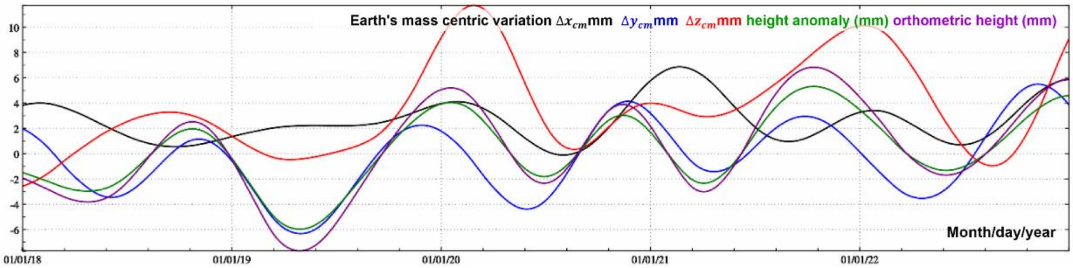


**Fig 5.11 The Earth's mass centric variation and their effect time series on the geoid and normal height at the ground point P**

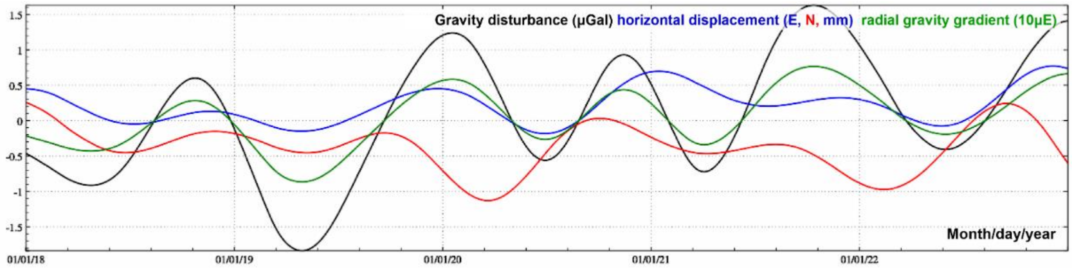


**Fig 5.12 The Earth's mass centric variation effect time series on the geodetic variations at the ground point P**

The Earth's center of mass is a typical geodetic element and its variation effects on various geodetic elements objectively exist, while the center of crustal shape is fictitious, and the geodetic elements are not affected by this fictitious center of crustal shape. So it is recommended to dilute the concepts of center of crustal shape and center of mass of solid Earth. In the calculation of the load Green's function integral and load spherical harmonic synthesis, only the Earth's mass centric load effects are considered, and the degree-1 load potential Love number is therefore always equal to zero, namely $k_1' \equiv 0$.

### 8.5.4 Earth's figure polar shift effects on all-element geodetic variations

The Earth's figure polar shift $\left(\Delta x_{sfp} = b\Delta\mu_1, \Delta y_{sfp} = -b\Delta\mu_2\right)$ can be determined by measuring the degree-2 tesseral harmonic geopotential coefficient variations $(\Delta\bar{C}_{20}, \Delta\bar{C}_{21})$ as follows:

$$\Delta\mu_1 = \frac{\Delta x_{sfp}}{b} = -\frac{\sqrt{3}}{\bar{C}_{20}}\Delta\bar{C}_{21}, \quad \Delta\mu_2 = -\Delta y_{sfp}/b = -\frac{\sqrt{3}}{\bar{C}_{20}}\Delta\bar{S}_{21} \tag{5.23}$$

Here, the geopotential coefficients $\bar{C}_{20}$ and $\bar{S}_{22}$ can be the mean values.

From Formula (5.23), we have:

$$\Delta\bar{C}_{21} = -\frac{\bar{C}_{20}}{\sqrt{3}b}\Delta x_{sfp}, \quad \Delta\bar{S}_{21} = \frac{\bar{C}_{20}}{\sqrt{3}b}\Delta y_{sfp} \tag{5.24}$$

Substitute Formula (5.24) into Formula (5.6), and have:

$$\Delta\bar{C}_{21}^{w} = -\frac{5\bar{C}_{20}}{3\sqrt{3}b}\frac{\rho_e}{(1+k_2')\rho_w}\Delta x_{sfp}, \quad \Delta\bar{S}_{21}^{w} = \frac{5\bar{C}_{20}}{3\sqrt{3}b}\frac{\rho_e}{(1+k_2')\rho_w}\Delta y_{sfp} \tag{5.25}$$

Then substitute the formula (5.25) into the formulas (2.8) ~ (2.20), and let n = 2, m = 1, considering $\bar{P}_{nm}(cos\theta) = \sqrt{15}sin\theta cos\theta$, we can obtain the algorithm formulas of the Earth's figure polar shift effects on geodetic variations from the measured figure polar shift. Among them, the algorithm formula of the Earth's figure polar shift effect on height anomaly at $(r,\theta,\lambda)$ is:

$$\Delta\zeta(r,\theta,\lambda) = -\frac{\sqrt{5}GMa^2}{2\gamma r^3}\frac{\bar{C}_{20}}{b}\left(\Delta x_{sfp}cos\lambda - \Delta y_{sfp}sin\lambda\right)sin2\theta \tag{5.26}$$

Where, $\bar{C}_{20}$ is the degree-2 zonal geopotential coefficient, and the approximate mean value is taken.

The algorithm formula of the Earth's figure polar shift effect on ground gravity is◉:

$$\Delta g^{s}(r,\theta,\lambda) = -\frac{3\sqrt{5}GMa^2}{2r^4}\frac{\bar{C}_{20}}{b}\frac{1-\frac{3k_2'}{2}+h_2'}{1+k_2'}\left(\Delta x_{sfp}cos\lambda - \Delta y_{sfp}sin\lambda\right)sin2\theta \tag{5.27}$$

Where, $k_2', h_2'$ are the degree-2 load potential and radial Love number, respectively.

The algorithm formula of the Earth's figure polar shift effect on gravity (disturbance) outside the solid Earth is:

$$\Delta g^{\delta}(r,\theta,\lambda) = -\frac{3\sqrt{5}GMa^2}{2r^4}\frac{\bar{C}_{20}}{b}\left(\Delta x_{sfp}cos\lambda - \Delta y_{sfp}sinm\lambda\right)sin2\theta \tag{5.28}$$

The algorithm formula of the Earth's figure polar shift effect on ground tilt is◉:

$$\text{South: } \Delta\xi^{s}(r,\theta,\lambda) = -\frac{\sqrt{5}GMa^2}{\gamma r^4}\frac{\bar{C}_{20}}{b}\frac{1+k_2'-h_2'}{1+k_2'}\left(\Delta x_{sfp}sin\lambda + \Delta y_{sfp}cos\lambda\right)cos\theta \tag{5.29}$$

$$\text{West: } \Delta\eta^{s}(r,\theta,\lambda) = -\frac{\sqrt{5}GMa^2}{\gamma r^4}\frac{\bar{C}_{20}}{b}\frac{1+k_2'-h_2'}{1+k_2'}\left(\Delta x_{sfp}cos\lambda - \Delta y_{sfp}sin\lambda\right)sin\theta cos2\theta \tag{5.30}$$

The algorithm formula of the Earth's figure polar shift effect on vertical deflection outside the solid Earth is:

$$\text{South: } \Delta\xi(r,\theta,\lambda) = -\frac{\sqrt{5}GMa^2}{\gamma r^4}\frac{\bar{C}_{20}}{b}\left(\Delta x_{sfp}sin\lambda + \Delta y_{sfp}cos\lambda\right)cos\theta \tag{5.31}$$

$$\text{West: } \Delta\eta(r,\theta,\lambda) = -\frac{\sqrt{5}GMa^2}{\gamma r^4}\frac{\bar{C}_{20}}{b}\left(\Delta x_{sfp}cos\lambda - \Delta y_{sfp}sin\lambda\right)sin\theta cos2\theta \tag{5.32}$$

The algorithm formula of the Earth's figure polar shift effect on ground site displacement is◉:

$$\text{East: } \Delta n(r,\theta,\lambda) = \frac{\sqrt{5}GMa^2}{\gamma r^3}\frac{\bar{C}_{20}}{b}\frac{l_2'}{1+k_2'}\left(\Delta x_{sfp}cos\lambda - \Delta y_{sfp}sin\lambda\right)sin\theta cos2\theta \tag{5.33}$$

$$\text{North: } \Delta e(r,\theta,\lambda) = \frac{\sqrt{5}GMa^2}{\gamma r^3}\frac{\bar{C}_{20}}{b}\frac{l_2'}{1+k_2'}\left(\Delta x_{sfp}sin\lambda + \Delta y_{sfp}cos\lambda\right)cos\theta \tag{5.34}$$

$$\text{Radial: } \Delta r(r,\theta,\lambda) = -\frac{\sqrt{5}GMa^2}{2\gamma r^3}\frac{\bar{C}_{20}}{b}\frac{h_2'}{1+k_2'}\left(\Delta x_{sfp}cos\lambda - \Delta y_{sfp}sin\lambda\right)sin2\theta \tag{5.35}$$

Where, $l_2'$ is the degree-2 load horizontal Love number.

The algorithm formula of the Earth's figure polar shift effect on gravity gradient outside the solid Earth is:

$$\text{Radial: } \Delta T_{rr}(r,\theta,\lambda) = -\frac{6\sqrt{5}GMa^2}{r^5}\frac{\bar{C}_{20}}{b}\left(\Delta x_{sfp}cos\lambda - \Delta y_{sfp}sin\lambda\right)sin2\theta \tag{5.36}$$

$$\text{North: } \Delta T_{NN}(r,\theta,\lambda) = \frac{2\sqrt{5}GMa^2}{r^5}\frac{\bar{C}_{20}}{b}\left(\Delta x_{sfp}cos\lambda - \Delta y_{sfp}sin\lambda\right)sin2\theta \tag{5.37}$$

$$\text{West: } \Delta T_{WW}(r,\theta,\lambda) = -\frac{\sqrt{5}GMa^2}{r^5}\frac{\bar{C}_{20}}{b}\left(\Delta x_{sfp}cos\lambda - \Delta y_{sfp}sin\lambda\right)ctg\theta \tag{5.38}$$

In the following, using the the degree-2 tesseral harmonic geopotential coefficient variation monthly time series (the 5 years of mean removed) from Center for Space Research in University of Texas in USA (UT/CSR) from LAGEOS-1/2, Stella, Starlette, AJISAI, BEC and LARES Satellite Laser Ranging (SLR) measured, the Earth's figure polar coordinate variation time series are calculated as shown in Fig 5.13.

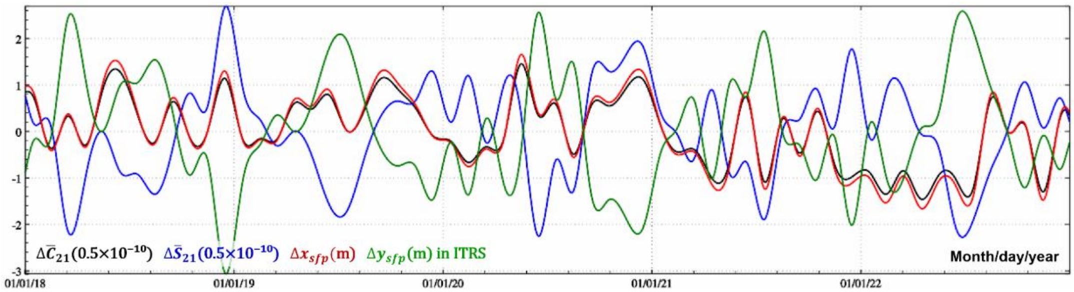


**Fig 5.13 The degree-2 tesseral harmonic geopotential coefficient and figure polar coordinate variation time series in ITRS from SLR measured**

Taking the degree-2 load Love number $k_2' = -0.3058$, $h_2' = -0.9946$ and $l_2' = 0.0241$, the Earth's short semi-axis $b$ = 6356751.655m and the degree-2 zonal harmonic geopotential coefficient $\bar{C}_{20} = -4.84165 \times 10^{-4}$, the time series of the Earth's figure polar shift effects on various geodetic elements at the ground point P (105.0°E, 32.0°N, H720m) are calculated according to formulas (5.26) ~ (5.38) from the coordinate variation time series of Earth's figure pole, as shown in Fig 5.14. The time span of the time series is from January 2018 to December 2022 (5 years).

Fig 5.14 shows that although the Earth's figure polar shift itself can reach the meter level, the resulting effect on geoid is not greater than 2mm. The Earth's figure polar shift effects on horizontal geodetic elements such as ground horizontal displacement, vertical deviation or horizontal gravity gradient are small and can be generally ignored.

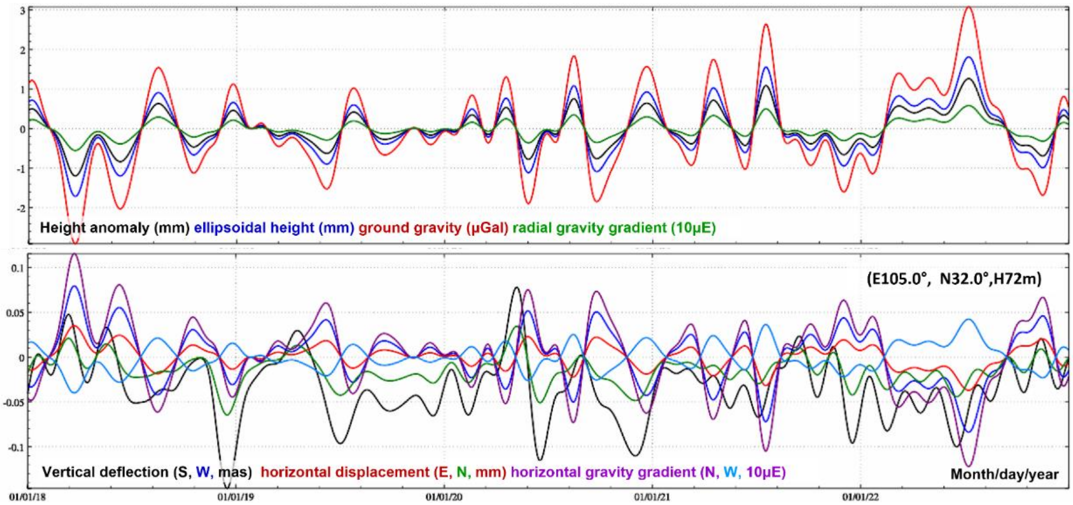


**Fig 5.14 The time series of Earth's figure polar shift effects on various geodetic elements at the point P**